Correlation between overgrowth morphology and optical properties of single self-assembled InP quantum dots

M. K.-J. Johansson,* U. Håkanson, M. Holm, J. Persson, T. Sass,† and J. Johansson
Solid State Physics/Nanometer Consortium, Lund University, P.O. Box 118, S-221 00 Lund, Sweden

C. Pryor
Optical Science and Technology Center, University of Iowa, Iowa City, Iowa 52242, USA

L. Montelius, W. Seifert, L. Samuelson, and M.-E. Pistol
Solid State Physics/Nanometer Consortium, Lund University, P.O. Box 118, S-221 00 Lund, Sweden
(Received 3 April 2003; published 4 September 2003)

We have studied the early stages of GaInP overgrowth on InP quantum dots (QD's) experimentally and theoretically. A direct correlation between the surface morphology and the optical properties of individual InP QD's is made using scanning tunneling microscopy (STM) and scanning tunneling luminescence. The geometric structure of the islands is further investigated using cross-sectional transmission electron microscopy (TEM). The overgrowth occurs in three stages; initially the InP QD's act as seeding points for the overgrowth, where the GaInP grows laterally from the side facets of the QD. The growth occurs preferentially in the [110] direction and elongated GaInP/InP islands are formed. As the overgrowth continues the islands increase laterally in size and GaInP also starts to grow between the islands, but not covering the top of the InP QD's. The growth of GaInP on top of the QD's commences once the islands have begun to coalesce. Using a model based on the STM and TEM results the electronic structures of the QD's have been calculated by eight-band $\mathbf{k}\cdot\mathbf{p}$ theory. The calculations are in good agreement with the experimental results. Our findings unravel the details of the strain induced energy shift of the QD luminescence previously reported [Pistol *et al.*, Appl. Phys. Lett. **67**, 1438 (1995)].

DOI: 10.1103/PhysRevB.68.125303 PACS number(s): 78.67.Hc, 78.60.−b, 68.37.Ef, 81.07.Ta

I. INTRODUCTION

Self-assembled semiconductor quantum dots (QD's) have been the subject of extensive studies in the last decade.[1] The interest stems from both science and technology, which have involved QD's in studies of the fundamental properties as well as for building blocks in optoelectronic devices.[2,3] The local environment of a QD has a considerable impact on the electronic structure both in terms of strain and confinement. Consequently, the effects of a thin capping layer have been investigated for a variety of QD systems, such as InAs/GaAs,[4–7] InGaAs/GaAs,[8–10] InSb/InP,[11] CdSe/ZnSe,[12] SiGe/Si,[13,14] and InP/GaInP.[15,16] For instance, Joyce *et al.*[6] have recently shown that GaAs growth on top of large InAs QD's formed at low growth rates is hampered, which leads to a reduction of the In segregation and In-Ga intermixing during the GaAs overgrowth.[17] For the same material system, Wang *et al.*[4] found that the use of InGaAs as a capping material reduced the surface strain, leading to a redshift of the photoluminescence (PL) emission with increasing In content. In an early study of InP/GaInP QD's by Pistol *et al.*,[15] it was shown that the GaInP cap layer thickness has a strong influence on the optical properties of the QD's. Intriguingly, the blueshift of the PL emission increased slowly for low cap thicknesses and at GaInP thickness of about 20 nm the blueshift exhibited a steep increase with further growth of the capping layer.

We have recently demonstrated the feasibility of using scanning tunneling microscopy (STM) and scanning tunneling luminescence (STL) to make a direct correlation between the morphology of the surface and the optical properties of semiconductor nanostructures.[18,19] For instance, we have shown that fully developed InP QD's act as templates in the formation of GaInP domains with a higher degree of ordering than that of the GaInP bulk.[16]

In the present study we have used STM, STL, and transmission electron microscopy (TEM) to follow the evolution of the surface morphology and the optical properties of single InP QD's as a function of GaInP overgrowth thickness. We find that GaInP initially only grows laterally from the side facets of the QD's and GaInP islands are formed, extending in the [110] direction. The lateral growth continues with further deposition, although competing with the layer-by-layer growth of GaInP in between the islands. Once the islands begin to merge the GaInP starts to grow on top of the QD's, which is found to be the onset for an enhanced blueshift of the QD emission with further increase of the capping layer thickness. The electronic structure has been calculated with eight-band $\mathbf{k}\cdot\mathbf{p}$ theory, in which a realistic model of the overgrowth was used, based on the structural information from the STM and TEM data. The calculations are in good agreement with the experiments and reveal that electron states, rather than hole states, are responsible for the observed evolution of the QD emission. Furthermore, we conclusively show that the change in rate of the blueshift is directly correlated to the onset of growth of GaInP on top of the InP QD's.

II. EXPERIMENTAL DETAILS

A. Sample preparation

The samples were grown by metal-organic vapor-phase epitaxy (MOVPE) using a low-pressure (100 mbar) rf-heated reactor. Trimethylgallium (TMG), trimethylindium (TMI), PH_3, AsH_3, and Si_2H_6 precursors were used with H_2 as the carrier gas. Initially, a 250-nm-thick $Ga_{0.51}In_{0.49}P$ (which we in the following refer to as GaInP) layer was grown, lattice matched to the (001)GaAs substrate, followed by two monolayers (ML) of GaP to increase the size homogeneity of the QD's.[20] The QD's were then grown in the Stranski-Krastanow mode by deposition of 3 ML (0.5 ML/s) InP at 580 °C. This was followed by a 12-s anneal, after which the samples were overgrown with nominally 5, 10, 20, or 30 nm of GaInP (0.33 nm/s) and subsequently cooled to room temperature. The GaInP was highly *n* doped (Si, $n = 10^{18}$ cm^{-3}). Using the growth conditions above, uncapped samples show fully developed, slightly truncated, QD's having heights between 12 and 15 nm and base widths of 40–50 nm and 55–65 nm in the $[\bar{1}10]$ and [110] directions, respectively. The density of QD's was measured on uncapped samples to be about 10^9 cm^{-2} by atomic force microscopy (AFM) and STM. It has previously been shown that the shape of the dots is not affected by the overgrowth.[21] Further details of the growth can be found elsewhere.[20,22]

In order to ensure stable tunneling conditions in the STM and STL measurements, the samples were sulfur passivated by immersion into a 2% ammonium sulfide solution kept at 55 °C for 30 min. The samples were then outgassed at 120 °C for 12 h in the load-lock chamber before transfer into the ultrahigh-vacuum (UHV) chamber of the STM.

The $[\bar{1}10]$ and [110] cross-section samples for the TEM investigations were prepared by cleaving, mechanical grinding, and polishing, followed by Ar^+-ion milling until electron transparency was reached.

B. Measurements

The STM and STL measurements were carried out using a variable-temperature UHV-STM, in which the samples can be cooled to 20 K. The STM tips were prepared from tungsten wires by electrochemical etching in a 2 mol/dm^3 KOH solution. Prior to the experiments, the tips were cleaned *in situ* by Ar^+-ion sputtering and radiative heating using a tungsten filament. The system is equipped with an optical detection system and a laser source, which allows for STL and PL to be performed without changing the sample position.[19] The PL was obtained using a frequency-doubled Nd:yttrium aluminum garnet (YAG) laser emitting at 532 nm. The luminescence signal was collected by a lens (50 mm in diameter), situated 100 mm from the tip-sample region, and focused onto the entrance slit of a 0.27-m monochromator. The dispersed emission was then detected using a liquid-nitrogen-cooled Si charge-coupled device (CCD) camera. A note about the STL measurements: STM images were acquired before and after acquisition of the STL spectra to ensure that no changes of the surface had occurred as well as to determine any drift. The tip positions indicated in the figures represent the mean positions during STL acquisition. The TEM examinations were performed using a JEOL 4000EX microscope with a point-to-point resolution of 0.16 nm, operated at an acceleration voltage of 400 keV.

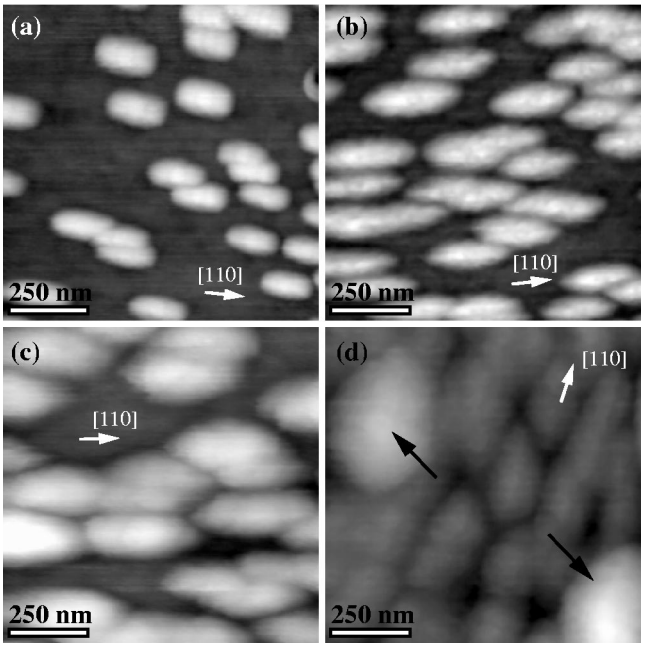

FIG. 1. STM constant-current topographs of InP QD's overgrown with nominally (a) 5 nm, (b) 10 nm, (c) 20 nm, and (d) 30 nm of GaInP. The images are 1×1 μm^2 in size and were acquired using a tunneling current of 100 pA and a sample bias of -6 V.

III. RESULTS AND DISCUSSION

A. Morphology and structure

Figure 1 shows STM constant current topographs of InP QD samples overgrown with nominally 5, 10, 20, and 30 nm of GaInP. In the case of a 5-nm cap [see Fig. 1(a)], bright dome-shaped features are clearly visible, corresponding to islands of partially overgrown InP dots. These GaInP/InP islands are rather uniform in size, having apparent heights of 12–15 nm and apparent widths of 100–130 nm and 190–220 nm in the $[\bar{1}10]$ and [110] directions, respectively. The large lateral size of the islands, as compared to uncapped QD's, indicates that the InP QD's act as seeding points for the GaInP capping layer and almost all of the material supplied during the overgrowth is incorporated into the islands. Furthermore, the height of the islands is approximately the same as for uncapped dots, which suggests that during the initial stages of the overgrowth, GaInP preferentially grows laterally from the side facets of the InP QD's (Ref. 19) and not on top of the QD's. The surface morphology has a similar appearance when the cap layer thickness is increased to 10 nm, although we observe an increase in the island sizes as well as a larger size distribution; cf. Fig. 1(b). The islands have typical heights of 9–11 nm and widths of 140–160 nm and 250–300 nm in the $[\bar{1}10]$ and [110] directions, respectively, but islands as large as 350 nm were occasionally observed. The increase in island size implies that a significant part of the

GaInP grows at the islands; however, the slight decrease in island height indicates that epitaxial growth of GaInP in between the QD's also occurs.

Increasing the cap layer thickness to 20 nm substantially alters the appearance of the surface. At this point islands have begun to merge [see Fig. 1(c)], although flat areas in between the islands are still observable where the QD nearest-neighbor distances are sufficiently large. The islands have typical heights of 8–11 nm and widths of 150–250 nm and 350–425 nm in the $[\bar{1}10]$ and [110] directions, respectively. The increase in lateral dimensions of the islands does not fully account for the supplied amount of material, and since the height of the islands is about the same as for the 10-nm cap layer, GaInP has most probably begun to grow on top of the InP QD's. Occasionally, large islands with heights of 20–27 nm and widths of about 300 nm and 400 nm, in the $[\bar{1}10]$ and [110] directions, respectively, were observed. In Fig. 1(d), QD's capped with nominally 30 nm of GaInP are shown. The surface morphology is complex; the GaInP/InP islands have coalesced and flat areas are rarely observed. The lateral sizes of the islands are smaller than in the case of a 20-nm cap layer because of the merge and their apparent dimensions are determined by the merger boundaries. The morphology observed is a manifestation of the growth of GaInP domains rather than of individual islands with an InP QD in the center. Hence, what appears to be an island in the STM topographs does not necessarily correspond to a single overgrown QD. In addition, larger-scale features are often seen with typical dimensions of 450–600 nm [indicated in Fig. 1(d) with black arrows], which are 20–35 nm higher than the neighboring islands. The occurrence of these larger islands will be further discussed below.

We have also used cross-sectional TEM to determine the structure of the overgrown material. The TEM data corroborate the STM experiments and provide further information, which strengthens the interpretation of how overgrowth occurs. Figure 2(a) shows a TEM micrograph of an InP QD after overgrowth of nominally 5 nm of GaInP. There is an evident interface (indicated by a white arrow) as an effect of differences in thickness, i.e., electron transparency, between the GaInP/InP island and the bulk GaInP. The island is 250 nm wide with a QD in the center, visible as a dark area due to the strain fields inside and in the proximity of the QD [see Fig. 2(b)]. Furthermore, the TEM image in Fig. 2(a) reveals that there is a small height modulation in the GaInP island: the GaInP in the vicinity of the QD (arrow *A*) is about 2 nm lower than the QD, but approximately 20 nm away from the QD, the GaInP is instead 2–3 nm higher than the QD (arrow *B*). This height modulation of the islands is still present when the nominal cap layer thickness is increased to 10 nm, which is shown in the TEM micrograph of Fig. 2(c). However, the size of the island is larger and, as suggested by our STM data, the TEM data show that even for a 10-nm-thick cap layer the top of the InP QD is not covered by GaInP [cf. Fig. 2(d)].

Figure 3(a) shows a TEM micrograph of two GaInP/InP islands that have coalesced at a nominal GaInP capping layer thickness of 20 nm. At this coverage, GaInP has begun to grow on top of the QD's, reaching a typical thickness of

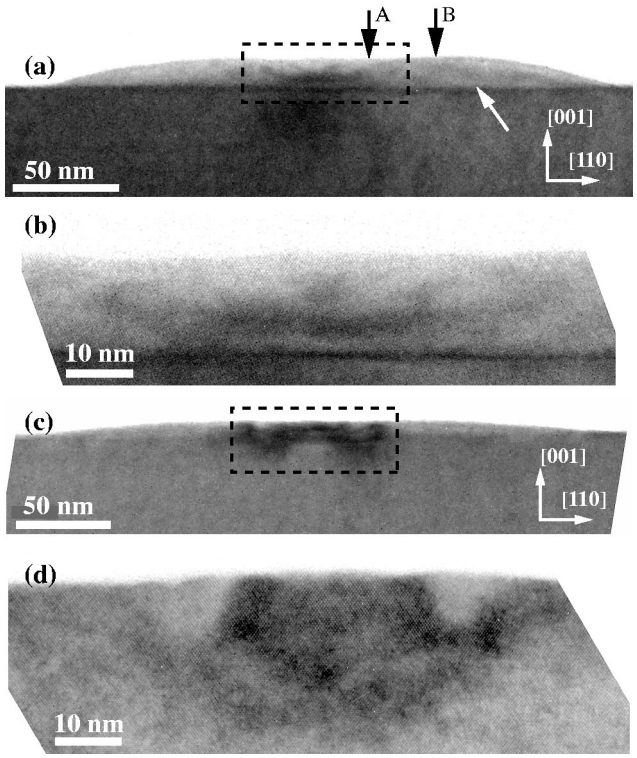

FIG. 2. Cross-sectional TEM micrographs of InP QD's overgrown with nominally (a), (b) 5 nm and (c), (d) 10 nm of GaInP. Enlarged views of the areas indicated by a dashed rectangle in (a) and (c) are shown in (b) and (d), respectively. Arrows *A* and *B* indicate regions in the GaInP/InP island with differing heights, which are discussed in the text.

about 8 nm. The presence of QD's in the islands is seen as darker gray areas in the micrograph due to the strain fields in and around the QD's. The sample is not cut through the center of the island to the left and thus the strain fields are not as pronounced as in the island to the right, for which the QD is indicated by a black arrow. Figures 3(b) and 3(c) show InP QD's capped with nominally 30 nm of GaInP, from which it is clear that the GaInP island shape does not necessarily reflect the positions of the InP QD's. Two common types of larger GaInP islands are observed, either with a QD in the center or with two QD's closer to the edge of the island [see Figs. 3(b) and 3(c), respectively]. In the latter case, the distance between the neighboring InP QD's is sufficiently small that the GaInP islands merge during an early stage of the overgrowth, after which the GaInP appears to grow preferentially in between the QD's. Notably, domains of ordered GaInP are formed during the overgrowth, having a double periodicity in the $[\bar{1}11]$ and $[1\bar{1}1]$ directions.[23] The QD-induced ordering for this particular material system has recently been discussed in detail in Refs. 16 and 23.

There is a rather complex interplay between the QD-QD distance and the growth of GaInP. The lateral width of a GaInP island does not provide any information whether it contains one or several QD's. However, there are some significant differences between the single-QD (SQD) and double-QD (DQD) islands. The SQD islands are higher, about 35 nm above the surface, as compared to the DQD

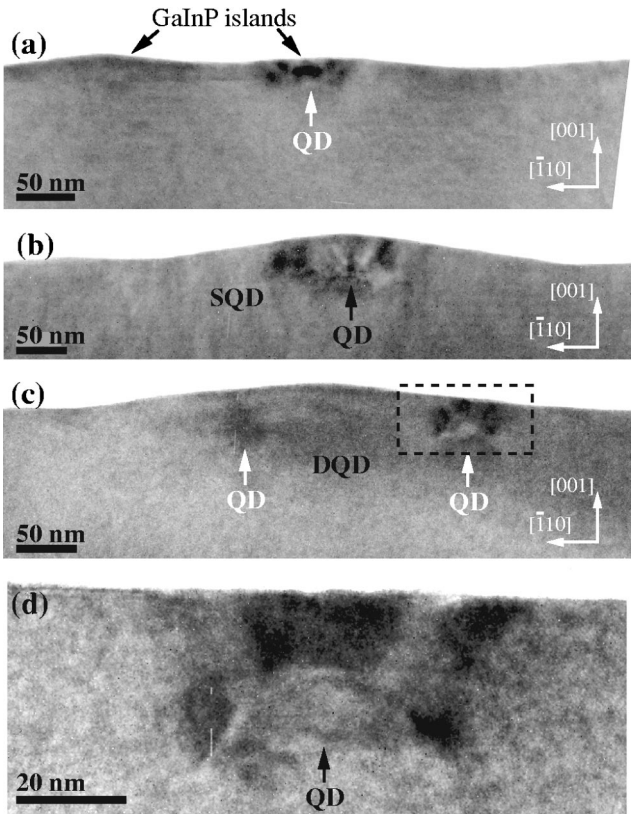

FIG. 3. Cross-sectional TEM micrographs of InP QD's overgrown with nominally (a) 20 nm and (b), (c) 30 nm of GaInP. (d) An enlarged view of the area indicated by the dashed rectangle in (c).

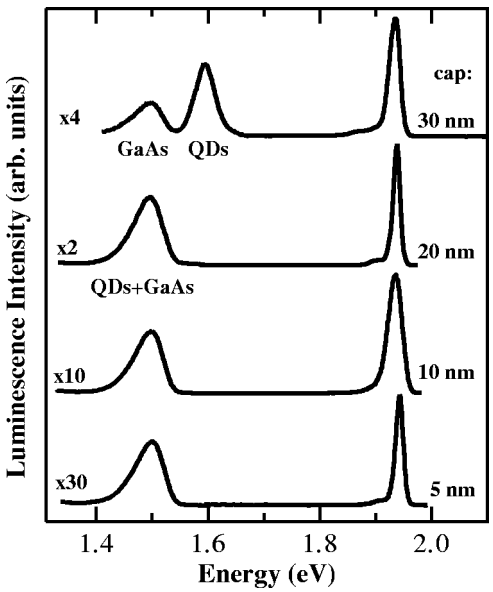

FIG. 4. *In situ* PL of InP QD's overgrown with nominally 5 nm, 10 nm, 20 nm, and 30 nm of GaInP. The measurements were performed at a sample temperature of 20 K.

islands, which typically have a height of about 22 nm. The SQD islands are also steeper in the $[\bar{1}10]$ direction, with an inclination of about 10° to the (001) plane as compared to 6° for DQD islands. In Fig. 3(d) a detailed view of the area indicated by a black rectangle in Fig. 3(c) is shown, in which an InP QD can be seen. We stress that the shape of the InP QD is retained during overgrowth as reported previously.[21] In addition, we do not see any evidence of an InP wetting layer, which is not surprising considering the possibility of intermixing between the GaP layer grown prior to the QD's and an InP wetting layer.

A summary of the TEM measurements is given in Table I. The island sizes found by TEM are comparable to the STM measurements of the different capping layer thicknesses investigated. Intriguingly, the TEM finds evidence that there has already been a considerable growth of GaInP in between the islands at a nominal cap layer of 10 nm. In addition, there is no GaInP on top of the QD at this nominal cap thickness, which the STM data suggested but could not conclusively show. The reluctance of GaInP to grow on top of the InP QD is not surprising considering the lattice mismatch between the (001) surfaces of InP and GaInP.

B. Optical properties

In Fig. 4 *in situ* PL spectra of the samples having different cap layer thicknesses are shown. For nominal GaInP thicknesses ranging from 5 nm to 20 nm the spectra have a very similar appearance with a strong emission peak at 1.94 eV from the GaInP matrix and a broad emission peak around 1.5 eV. The latter peak is attributed to the superpositioned emission from the GaAs substrate and from a large ensemble of QD's. At a nominal thickness of 30 nm the emission from the QD's has shifted towards higher energies, giving rise to an additional peak at 1.6 eV, as an effect of the strain induced by the cap layer.[15] The QD emission is well defined, implying that the QD ensemble has a fairly homogeneous distribution in size and shape. Since the surface density of the QD's is too high to allow for PL of single QD's using a conventional μ-PL setup and the emissions from the QD's

TABLE I. Summary of the TEM measurements.

Nominal Cap	Island dimensions (nm)			GaInP thickness (nm)	
(nm)	height	length$_{[\bar{1}10]}$	length$_{[110]}$	above QD	islands
5	13–14	149	251	0	0
10	13–14	181	307	0	5–6
20	20	240	541	8–9	10–12
30	30–49	418	–	19–38	20–23

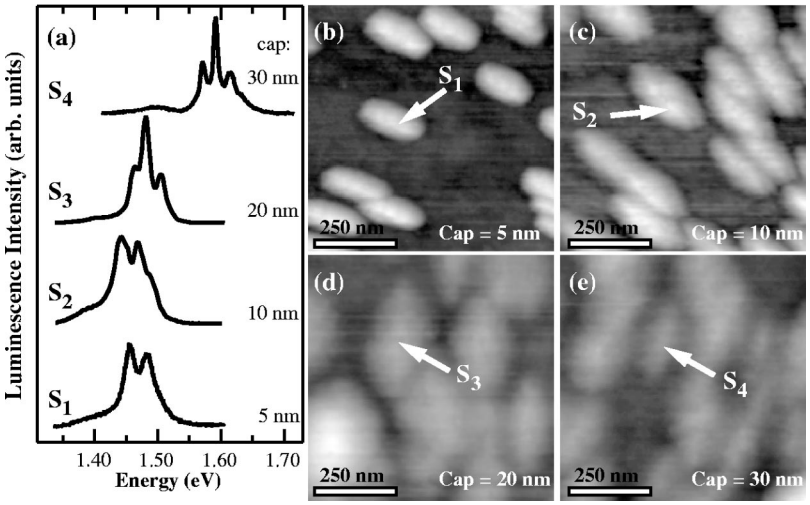

FIG. 5. (a) Scanning tunneling luminescence spectra from individual QD's and (b)–(e) the corresponding constant current topographs. The measurements were made at a sample temperature of 20 K, using a sample bias of −6 V. The tunneling current was 100 pA during imaging and 20, 5, 5, and 20 nA during acquisition of spectra S_1, S_2, S_3, and S_4, respectively. The arrows in the STM images indicate the tip position during the STL measurements.

and the GaAs substrate coincide for the lower nominal cap thicknesses, we have utilized the STM tip as a local excitation source.

In all the measurements presented below the sample was negatively biased relative to the tip. Under these conditions the Fermi level of the tip is below the valence band edge of the sample, from which electrons are extracted, equivalent to injecting holes. The injected minority charge carriers recombine in the sample and photons are emitted.[24]

Figure 5(a) shows the evolution of single dot STL spectra as the nominal capping layer thickness is increased from 5 nm to 30 nm. It should be noted that the STL spectra in Fig. 5 constitute an excerpt from a large number of measurements on 60 different single QD's. However, the spectra represent the most commonly observed emission shapes and energies for the different cap layer thicknesses. The GaInP/InP islands, from which the spectra were obtained, are shown in the STM topographs of Figs. 5(b)–5(e). The tip positions are indicated by white arrows. Notably, if the tip were positioned in between QD's at a distance of approximately 200 nm from the nearest QD, no or only a very weak luminescence signal from QD's could be detected (nor any luminescence from the GaAs substrate), as has been shown in our earlier studies.[19,18]

At a nominal GaInP coverage of 5 nm a characteristic QD emission having an energy of about 1.46 eV is observed, in agreement with earlier PL results.[15] The QD emission is distributed over almost 150 meV and has two prominent peaks at 1.46 eV and 1.48 eV with almost equal intensity and a long emission tail extending towards lower energies; see spectrum S_1 in Fig. 5(a). There is also an evident asymmetry towards higher energies. In peak fitting of the spectrum, using Lorenzian line shapes of fixed width, a best fit requires an additional third emission peak at 1.50 eV. When the nominal cap layer thickness is increased to 10 nm a similar line shape is observed (see spectrum S_2), in which two emission peaks are clearly resolved at an energy of 1.44 eV and 1.47 eV, respectively.

However, at a nominal cap thickness of 20 nm the spectrum S_3 is substantially different as compared to lower nominal cap thicknesses. Three well-defined and pronounced emission peaks at 1.46 eV, 1.48 eV, and 1.51 eV are observed, for which a Lorenzian fit gives a full width at half maximum (FWHM) of 15 meV. There is a small blueshift in emission energy as compared to the lower nominal cap thicknesses and the overall shape of the emission has changed drastically, where the second emission peak has almost twice the intensity compared to the other peaks. Based on our STM and TEM data we estimate that there are 6–8 nm (Ref. 31) of GaInP on top of the QD. The line shape of the QD emission is similar when the nominal GaInP cap thickness is increased to 30 nm. However, the QD emission has shifted significantly towards higher energies. The GaInP overlayer on the QD in Fig. 5(e) is estimated to be 10–12 nm thick. In the STL spectrum S_4, three peaks at 1.57 eV, 1.59 eV, 1.62 eV and a clear shoulder at a higher energy are observed. Surprisingly, even though STL provides a very local excitation of the sample, emission from the GaAs substrate is observed. However, since the GaAs emission approximately scales with the luminescence intensity of the QD's and since the GaInP is transparent for the QD emission, we attribute the signal from the GaAs to arise from photoexcitation by the QD emission.[18]

The spectra in Fig. 5 have been fitted using Lorenzian line profiles, in which a fixed FWHM for the peaks in each spectrum were used. With this constraint a good fit was obtained for all nominal cap thicknesses except for the 30-nm capping layer. In this case, a good fit could not be achieved unless the FWHM were allowed to vary between the individual peaks. This suggests that there are more components than the four considered; however, these could not be unambiguously determined. The results are summarized in Table II and will be further discussed below.

As discussed in Sec. III A, we encountered significant variations in the overlayer thickness for the samples with larger nominal capping and, in particular, for the 30-nm case. An example of how these variations affect the optical properties of the QD's is shown in Fig. 6(a). The STL spectra were acquired with the STM tip at the positions indicated by the arrows in Figs. 6(b) and 6(c), at a sample temperature of 80 K. Spectrum P_1 is acquired with the STM tip positioned on top of a GaInP island of similar height compared to neighboring islands. The island, from which P_2 is obtained, is about 32 nm higher than neighboring QD's and its sides are

TABLE II. Summary of Lorenzian peak fitting of the scanning tunneling luminescence spectra in Fig. 5.

Nominal cap (nm)	E_1 (eV)	E_2 (eV)	E_3 (eV)	E_4 (eV)	FWHM (meV)	$\Delta(E_2-E_1)$ (meV)
5	1.456	1.484	1.502	–	22	28
10	1.442	1.470	1.490	–	25	28
20	1.462	1.481	1.506	–	15	20
30	1.571	1.592	1.617	1.635	9–27 [a]	20

[a]A best fit was obtained using FWHM values of 13, 9, 20, and 27 meV for peaks E_1, E_2, E_3, and E_4, respectively.

inclined by 12° to the surface in the $[\bar{1}10]$ direction, suggesting that this is an SQD island. There is a 52-meV shift of the emission peak towards higher energies for the spectra from the SQD island due the difference in GaInP cap thickness, i.e., strain excessed by the overgrowth.

A few general observations concerning the emission in the STL measurements can be made. All spectra have a fairly wide emission, which in the case of the QD's at the surface (i.e., for a nominal cap thickness of 5 and 10 nm) are distributed over almost 150 meV. For higher nominal cap thicknesses the emission is somewhat narrower but still in the order of 100 meV. Additionally, the low-energy tail present in the spectra from the surface QD's diminishes as the nominal cap thickness is increased. Although the low-energy emission tail seems related to the surface or the reduced tip-QD distance, its origin is presently not known. If we compare the FWHM of the two lowest-energy peaks from each spectra, E_1 and E_2 in Table II, it is clear that the peaks become more narrow for the buried QD's. We note that Hess *et al.*[25] made similar observations for QD structures in quantum wells, where a broadening was seen for QD's closer to the surface. Furthermore, we can compare our data with recent μ-PL measurements of individual QD's in the same material system. Hessman *et al.*[26,27] have studied fully developed, fully strained, single InP QD's, where an emission range of about 50 meV was reported. The broad emission was attributed to the presence of a large number of occupied electron states in the InP dot,[27] due to the surrounding *n*-type GaInP. In comparison with our results, using the spectrum obtained for the 30-nm case [S_4 in Fig. 5(a)], it is evident that the spectra have a very similar shape although the STL emission is broader and shifted due to the difference in capping layer thicknesses. Even though our samples have higher *n*-type doping, an argument based on the electron occupancy of the QD's does not explain the peak widths observed here. This issue needs be investigated further and here we can only speculate that charge fluctuations in the InP QD due to the presence of the STM tip or the nature of the excitation may play an important role.[28]

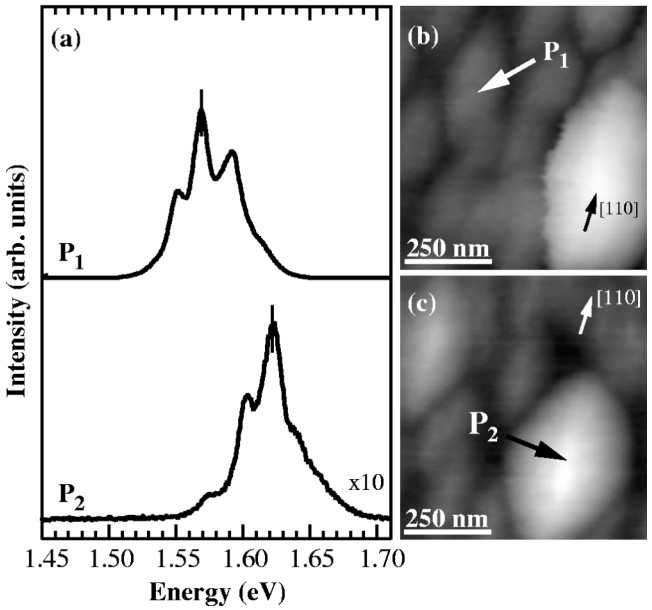

FIG. 6. STL and STM of GaInP/InP islands for a nominal capping layer thickness of 30 nm. (a) Scanning tunneling luminescence spectra from the GaInP/InP islands indicated in (b) and (c), respectively. The measurements were performed at a sample temperature of 80 K, using a sample bias of −6 V. The tunneling current was 100 pA during imaging and 20 nA during acquisition of STL spectra.

C. Theory

In addition to our experimental work, we have investigated the effects of capping layer thickness on the transition energies of InP QD's in GaInP using eight-band $\mathbf{k}\cdot\mathbf{p}$ theory in the envelope function approximation. Single-particle energies were calculated by first finding the strain profile using the finite-element method, followed by a diagonalization of the Hamiltonian using the Lanczos' algorithm. Details of the method can be found elsewhere.[29,30]

Investigations by TEM and STM (see Sec. III A) show that the overgrowth can be divided into three distinct modes according to the amount of capping material deposited. In the first mode, the overgrowth extends laterally, but does not cover the top of the QD. We have modeled this growth mode by an ellipsoid of capping material, with height equal to that of the QD [cf. Figs. 7(a) and 7(b)]. The ratio of the lateral dimensions of the ellipsoid was kept fixed to the experimentally measured size, 116 nm and 212 nm in the $[\bar{1}10]$ and [110], respectively, at an overgrowth corresponding to a nominal cap layer thickness of 5 nm. In the second growth mode, the overgrowth still extends laterally but material also accumulates layer by layer between the QD's. We treat this mode on an equal footing with the first growth mode, since the material that grows between the GaInP/InP islands does not effect the strain experienced by the QD's. The third growth mode is characterized by vertical growth [see Fig. 7(c)], with no further growth in the lateral direction beyond that obtained during the first two growth modes. We modeled this by increasing the height of the ellipsoid while keeping the lateral dimensions fixed. In the calculations we have used a QD with a height of 14 nm and a base width of 44 nm and 62 nm in the $[\bar{1}10]$ and [110] directions, respectively. In the discussion that follows we will refer to the first and second modes as the lateral growth mode G_L and the third mode as the vertical growth mode G_V.

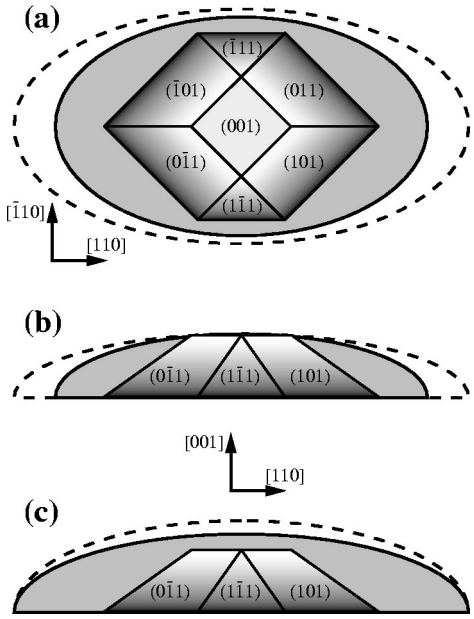

FIG. 7. Schematic drawings of the QD and cap geometries used in the calculations. (a) Projection on the (001) plane. (b), (c) Projection on the $(\bar{1}10)$ plane showing the lateral growth mode and the vertical growth mode, respectively. The dashed lines indicate the change in capping geometries for the growth modes.

Figure 8 shows band diagrams along the [001] direction computed using the local values of the strain and $\mathbf{k}=0$ for a QD with a nominal capping layer thickness of 5 nm, i.e., no capping material on top, and with 5 nm of capping material covering the QD (which corresponds to a nominal thickness of 23 nm; see below). The main difference between the two cases is the confining potential for the holes. With no capping material on top there is a shallow potential minimum (valence band maximum) around the base of the dot, while capping material causes a relatively deep potential well located above the QD in the GaInP cap. This minimum is induced by the heavily strained layers of capping material on the top surface of the QD. The potential profile experienced by the electrons is not significantly altered by the presence of capping material.

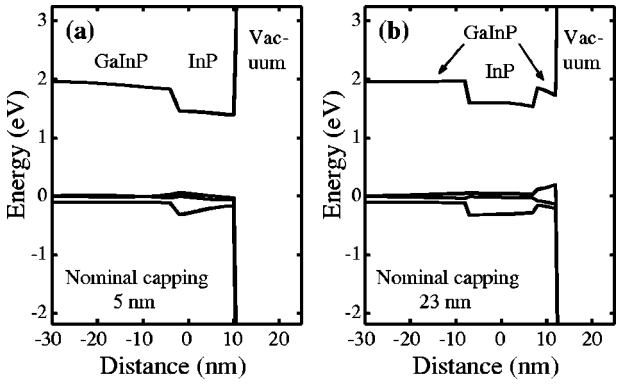

FIG. 8. Band diagrams through the center of a QD in the [001] direction with (a) a nominal capping layer thickness of 5 nm, i.e., no capping material on top, and (b) capped with 5 nm GaInP on top.

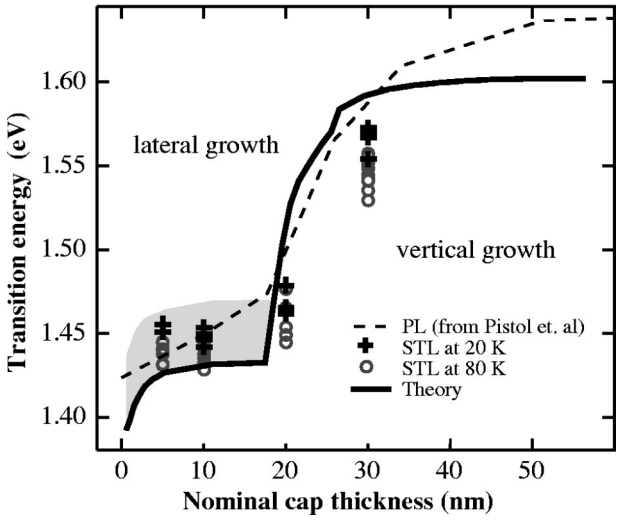

FIG. 9. Theroretical and experimental ground-state emissions as a function of capping layer thickness. The PL data is reproduced from Pistol *et al.* (Ref. 15).

We also calculated the electronic states for the capped QD's. First we computed ground-state electron and hole states keeping the height of the ellipsoid constant and equal to the height of the QD while the lateral dimension of the ellipsoid was varied (mode G_L). Second, we calculated the electron and hole ground states as a function of the ellipsoid's height (mode G_V) with the lateral dimensions held fixed at a sufficiently large size that the transition energy had converged for the mode G_L structure. This size corresponds to 224 nm and 418 nm in the $[\bar{1}10]$ and [110] directions, respectively. In the first case we parametrized the size of the ellipsoid by an equivalent planar capping layer thickness. By assuming each QD has access to an area A from which the deposited capping material of thickness t is collected, we have

$$At = V_{ellipsoid} - V_{dot}, \tag{1}$$

where $V_{ellipsoid}$ is the volume of the ellipsoid and V_{dot} is the volume of the QD. The parameter A was fitted to STM data for a GaInP/InP island at a nominal capping layer thickness of 5 nm, giving $A \approx 160 \times 160$ nm^2.

For the vertical growth mode we had to choose a lateral size for the ellipsoid beyond which the capping material accumulated on top of the QD rather than on the sides. The point at which growth crossed over from mode G_L to mode G_V was fitted to experiment, i.e., a nominal capping layer thickness of 18 nm as determined by TEM and STM (see Sec. III A), and for each extra nanometer of capping material deposited we assumed the height of the ellipsoid grew by the same amount. Figure 9 shows the calculated transition energies as a function of capping layer thickness, the PL data of Ref. 15, and the energies of the first emission peak as determined by STL from 60 different GaInP/InP islands. The shaded region in Fig. 9 indicates the transition energy difference between mode G_L and the equivalent calculation but with 1 nm of GaInP on top of the InP QD. The calculation is in good agreement with experiments and demonstrates that

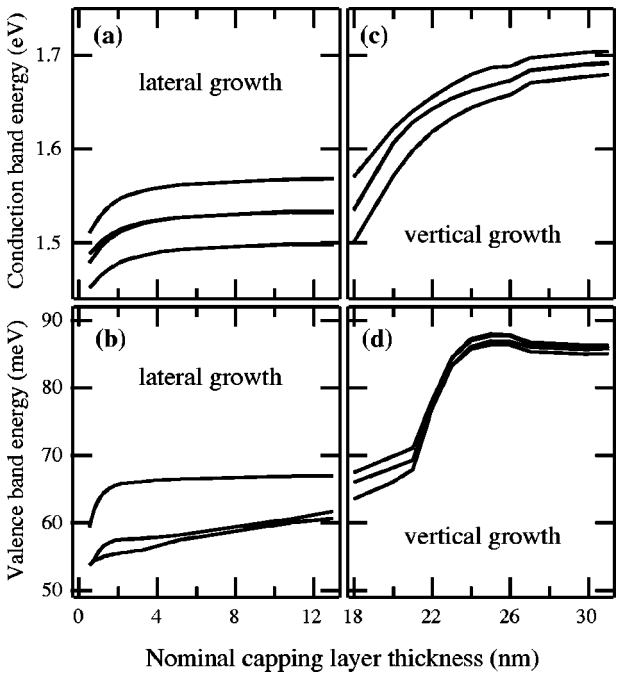

FIG. 10. Calculated energies of the four lowest electron states and four highest hole states as a function of GaInP capping. (a) Conduction and (b) valence band energies during the lateral growth. (c) Conduction and (d) valence band energies as a function of GaInP growth on top of the QD, i.e., vertical growth.

the strain-induced energy shift is highly dependent on the growth mode. In particular, the calculations conclusively show that the onset of enhanced blueshift of the QD emission is directly correlated to the beginning of GaInP growth on top of the QD.

Figure 10 shows electron and hole energies for the two growth modes. The calculations of the eigenvalues as a function of capping layer thickness show that the ground-state electron and hole energies increase 50 meV and 7 meV, respectively, when the nominal capping layer increases from 0 nm to 12 nm [mode G_L; cf. Figs. 10(a) and 10(b)]. When the nominal capping of the QD's increases from 18 nm to 30 nm [mode G_V, Figs. 10(c) and 10(d)] the ground-state electron and hole energies increase 170 meV and 22 meV, respectively, giving an increase in transition energy of 148 meV. Hence, we can conclude that the major contribution to the increase in transition energy with increasing capping layer thickness is the increase in electron energy. In addition, we note that the energy difference between the ground and first excited electron states decreases from 34 meV to 15 meV as the nominal cap thickness is increased from 5 nm to 30 nm. Comparing with the measured peak separations $\Delta(E_2-E_1)$ of 28 meV and 20 meV (cf. Table II), we find good agreement between theory and experiment.

IV. SUMMARY AND CONCLUSION

The evolution of the surface morphology during GaInP overgrowth of InP QD's has been studied by STM and TEM. In addition, the optical properties were studied by STL, which in combination with STM provides a direct correlation to the overgrowth morphology. The growth of GaInP on InP QD's can be divided into three distinct stages. During the initial stage GaInP grows solely laterally from the side facets of the QD's, forming islands elongated in the [110] direction. The second stage is characterized by the epitaxial growth of GaInP in between the islands in addition to the lateral growth of the GaInP/InP islands. In the third stage GaInP grows on top of the InP QD's. The transition between lateral (stages 1 and 2) and vertical (stage 3) growth is found to be the onset for the enhancement of the blueshift of the InP QD emission and is further characterized by the narrowing of individual emission peaks as well as a reduction of the peak separation. The electronic structure has been calculated using eight-band $\mathbf{k}\cdot\mathbf{p}$ theory, in which a realistic model for the overgrowth was used, based on experimental data. The calculations are in good agreement with the STL measurements and show that the electron states are responsible for the magnitude of the strain-dependent energy shift, induced by the overgrowth. We conclusively show that the change in rate of the blueshift is directly correlated to the onset of growth on top of the InP QD's.

ACKNOWLEDGMENTS

We gratefully acknowledge Claes Thelander for AFM measurements. Dr. Struan Gray is gratefully acknowledged for fruitful discussions and for comments on the manuscript. In addition, we acknowledge the financial support by the Swedish Foundation for Strategic Research (SSF), The Swedish Research Council (VR), The Wallenberg Foundation, and the ELFA Research Foundation. This work was performed within the Nanometer Consortium, Lund University.

*Corresponding author. Electronic address: mikael.johansson@ftf.lth.se
†Presently at: OSRAM Opto Semiconductors GmbH, Wernerwerkstr. 2, D-93049, Regensburg, Germany.

[1] See, for instance, D. Bimberg, M. Grundmann, and N.N. Ledentsov, *Quantum Dot Heterostructures* (Wiley, Chichester, 1999).
[2] Y.M. Manz, O.G. Schmidt, and K. Eberl, Appl. Phys. Lett. **76**, 3343 (2000).
[3] For a recent review see Z. Alferov, IEEE J. Sel. Top. Quantum Electron. **6**, 832 (2000).
[4] X.D. Wang, Z.C. Niu, and S.L. Feng, Jpn. J. Appl. Phys., Part 1 **39**, 5076 (2000).
[5] H.Y. Liu *et al.* J. Appl. Phys. **88**, 3392 (2000).
[6] P.B. Joyce, T.J. Krzyzewski, G.R. Bell, and T.S. Jones, Appl. Phys. Lett. **79**, 3615 (2001).
[7] P.B. Joyce, E.C. Le Ru, T.J. Krzyzewski, G.R. Bell, R. Murray, and T.S. Jones, Phys. Rev. B **66**, 075316/1 (2002).
[8] H. Saito, K. Nishi, and S. Sugou, Appl. Phys. Lett. **73**, 2742 (1998).
[9] L. Jeong-Sik, R. Hong-Wen, S. Sugou, and Y. Masumoto, J. Appl. Phys. **84**, 6686 (1998).

[10] D. Bhattacharyya, A. Saher Helmy, A.C. Bryce, E.A. Avrutin, and J.H. Marsh, J. Appl. Phys. **88**, 4619 (2000).
[11] J.A. Prieto, G. Armelles, T. Utzmeier, F. Briones, J.C. Ferrer, F. Peiro, A. Cornet, and J.R. Morante, Phys. Rev. Lett. **80**, 1094 (1998).
[12] X.B. Zhang and S.K. Hark, J. Electron. Mater. **30**, 1338 (2001).
[13] G. Patriarche, I. Sagnes, P. Boucaud, V. Le Thanh, D. Bouchier, C. Hernandez, Y. Campidelli, and D. Bensahel, Appl. Phys. Lett. **77**, 370 (2000).
[14] A. Hesse, J. Stangl, V. Holy, T. Roch, G. Bauer, O.G. Schmidt, U. Denker, and B. Struth, Phys. Rev. B **66**, 085321 (2002).
[15] M.-E. Pistol, N. Carlsson, C. Persson, W. Seifert, and L. Samuelson, Appl. Phys. Lett. **67**, 1438 (1995).
[16] U. Håkanson, T. Sass, M.K.-J. Johansson, M.-E. Pistol, and L. Samuelson, Phys. Rev. B **66**, 235308 (2002).
[17] D. Zhi, H. Davock, R. Murray, C. Roberts, T.S. Jones, D.W. Pashley, P.J. Goodhew, and B.A. Joyce, J. Appl. Phys. **89**, 2079 (2001).
[18] U. Håkanson, M.K.-J. Johansson, M. Holm, W. Seifert, L. Samuelson, and M.-E. Pistol, Appl. Phys. Lett. **81**, 4443 (2002).
[19] U. Håkanson, M.K.-J. Johansson, J. Persson, J. Johansson, M.-E. Pistol, L. Montelius, and L. Samuelson, Appl. Phys. Lett. **80**, 494 (2002).
[20] N. Carlsson, K. Georgsson, L. Montelius, L. Samuelson, W. Seifert, and R. Wallenberg, J. Cryst. Growth **156**, 23 (1995).
[21] K. Georgsson, N. Carlsson, L. Samuelson, W. Seifert, and L.R. Wallenberg, Appl. Phys. Lett. **67**, 2981 (1995).
[22] N. Carlsson, W. Seifert, A. Petersson, P. Castrillo, M.-E. Pistol, and L. Samuelson, Appl. Phys. Lett. **65**, 3093 (1994).
[23] U. Håkanson, V. Zwiller, M.K.-J. Johansson, T. Sass, and L. Samuelson, Appl. Phys. Lett. **82**, 627 (2003).
[24] A. Gustafsson, M.-E. Pistol, L. Montelius, and L. Samuelson, J. Appl. Phys. **84**, 1715 (1998).
[25] H.F. Hess, E. Betzig, T. Harris, L. Pfeiffer, and K. West, Science **264**, 1740 (1994).
[26] D. Hessman, P. Castrillo, M.-E. Pistol, C. Pryor, and L. Samuelson, Appl. Phys. Lett. **69**, 749 (1996).
[27] D. Hessman, J. Persson, M.-E. Pistol, C. Pryor, and L. Samuelson, Phys. Rev. B **64**, 233308 (2001).
[28] C. Obermüller, A. Deisenrieder, G. Abstreiter, K. Karrai, S. Grosse, S. Manus, J. Feldmann, H. Lipsanen, M. Sopanen, and J. Ahopelto, Appl. Phys. Lett. **74**, 3200 (1999).
[29] M. Holm, M.-E. Pistol, and C. Pryor, J. Appl. Phys. **92**, 932 (2002).
[30] C. Pryor, J. Kim, L.W. Wang, A.J. Williamson, and A. Zunger, J. Appl. Phys. **83**, 2548 (1998).
[31] The estimate is made as follows: the height of the GaInP/InP island above the GaInP surface, in between the islands, is measured in the STM image. The thickness of the GaInP on top of the QD is then calculated using the values of QD height and GaInP thickness between islands obtained from Table I.